INFLUENCE OF VOIDS ON THICK DCB JOINT BEHAVIOR

Jialiang Fan[1], Anastasios P. Vassilopoulos[2] and Veronique Michaud[3]

[1] Laboratory for Processing of Advanced Composites (LPAC),
Ecole Polytechnique Fédérale de Lausanne (EPFL), Lausanne, Switzerland,
jialiang.fan@epfl.ch, https://www.epfl.ch/labs/lpac/
[2] Composite Construction Laboratory (CCLab),
Ecole Polytechnique Fédérale de Lausanne (EPFL), Lausanne, Switzerland,
anastasios.vassilopoulos@epfl.ch, https://www.epfl.ch/labs/cclab/
[3] Laboratory for Processing of Advanced Composites (LPAC),
Ecole Polytechnique Fédérale de Lausanne (EPFL), Lausanne, Switzerland,
veronique.michaud@epfl.ch, https://www.epfl.ch/labs/lpac/

Keywords: DCB, Thick joints, Voids

ABSTRACT

The influence of voids on the quasi-static Mode I fracture performance of thick adhesive joints was investigated in this article. Double Cantilever Beam (DCB) joints were manufactured with glass fiber reinforced epoxy adherends and SikaPower®-830 epoxy adhesive in the cm thickness range. The high-viscosity adhesive leads to the inevitable presence of voids, resulting in unstable propagation and promoting crack path deviations. Voids could also decrease the apparent fracture strain energy release rate (SERR) since the SERR calculation assumes that the fracture surface contains no voids, while the actual surface area is reduced because of the voids. In conclusion, grooved DCB joints with low void content tested at low displacement rates showed stable crack propagation without significant crack path deviations, allowing the estimation of reliable materials fracture data.

1 INTRODUCTION

Over the past years, wind energy has consistently increased its market share [1]. The goal of reducing energy cost has driven the development of larger wind turbine rotor blades (WTRBs), which can reach or exceed 100 meters in length [2], [3]. WRTBs are typically manufactured by joining multiple composite components together using structural adhesives. The thickness of the bondline, which varies along the length of the blade, is typically within the centimeter range due to the massive size of these structures. However, there is a lack of research on the fracture behavior of adhesive joints with thick adhesive layers, and the few existing studies only focus on Mode I fracture because of the simple test configuration, and all reported experimental difficulties [4]–[7].

DCB joints have been commonly employed to study the Mode I fracture behavior of thin adhesively bonded joints with metallic and composite adherends [8]. However, applying the appropriate standards and experimental techniques to analyze thick adhesive joint configurations brings additional challenges: during such tests, crack propagation deviation towards the adherend surfaces and unstable crack propagation are generally observed, which complicate the investigation and raise doubts about the interpretation of results obtained, making it challenging to derive meaningful fracture data.

The voids within the thick adhesive layer are also a cause of these undesired phenomena. The existence of voids could influence the stress state ahead of the crack tip and lead to crack propagation deviation, or to a change in the crack propagation rate [9]. Moreover, voids could lead to bonding area decrease and stress concentration causing premature failure. For instance, Florian et al. [10] performed sub-component tests and established that a single defect was not detrimental, while the presence of multiple defects would diminish the fatigue lifetime of the component. Despite the existence of research on the effect of voids on the fracture behavior of joints, only a limited number of researchers have been able to derive conclusions from systematic investigations into their influence. The majority of studies on this topic have mostly focused on examining the impact of a single void on the behavior of thin

adhesive joints. As a result, the influence of void content on the fracture behavior of thick adhesive joints requires further investigation [11]–[13].

The presence of significant voids is a typical occurrence within thick adhesive layers [14], [15]. Thick adhesive joints are produced using high-viscosity, and high-yield-stress epoxy pastes. Despite various proposed methods for avoiding large voids, including mixing under vacuum and centrifuging the adhesive mixture, these approaches are still inadequate in eliminating all the internal voids because of the joint size, viscosity and manufacturing process [16], [17].

The influence of voids on thick DCB joint's fracture behavior is investigated in the present work, focusing on the overall void content as opposed to individual void discussed in previous literature.

2 MATERIALS AND METHODS

2.1 Materials and joint manufacturing

DCB joints were composed of glass fiber reinforced epoxy adherend and epoxy adhesive. Cross-ply laminates $[90/0]_{7S}$ with an average thickness of ca. 9.5 mm were manufactured using unidirectional glass fiber with vacuum assisted infusion process. The epoxy resin and hardener were EPIKOTE™ Resin MGS RIMR 135 and EPIKOTE™ Resin MGS RIMH 137 respectively. Composite plates were cured at room temperature for 24 hours and then underwent a post-curing process, which involved a temperature ramp for 2 hours from 20 °C to 60 °C, followed by 9.5 hours at 60 °C, and finally 6 hours at 80 °C.

The Sikapower®-830 (SP830) adhesive used for the joints was supplied by Sika technology AG. This two-part epoxy adhesive is specifically designed for wind turbine blade fabrication. The curing process for this adhesive involves heating it to 70 °C for four hours, as specified in the datasheet. To calculate the SERR, the elastic modulus of both the adherend and the adhesive was determined through a tensile test in accordance with ASTM D3039 and D638 standards separately [19], [20].

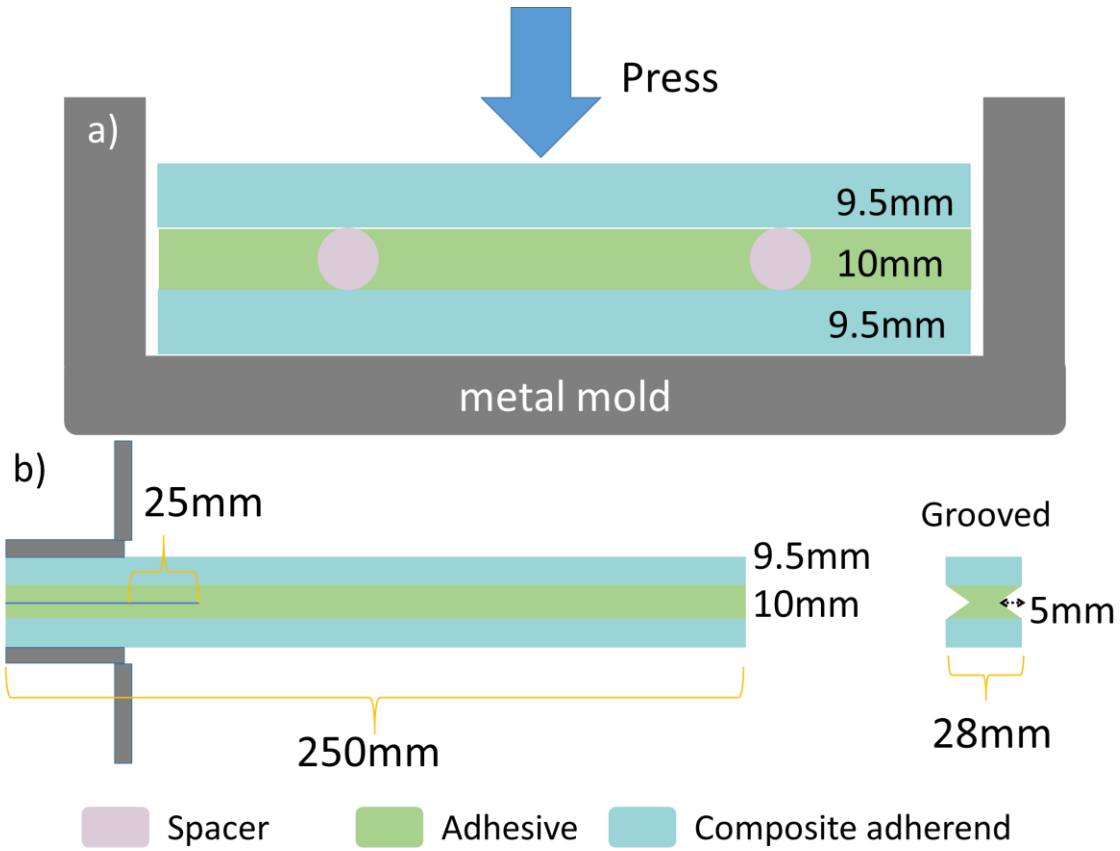

Figure 1: Illustration of the joint manufacturing method by applying enough pressure to control the void content: a) joint manufacturing under press; b) specimen before test.

Figure 1a illustrates the joint fabrication method, which is used for controlling the void content. Before mixing the epoxy adhesive, round spacers were glued to the bottom adherends. Then, hand-mixed adhesive was poured inside the remaining cavity. Following the placement of the top adherend, adequate pressure was applied to eliminate excess adhesive and reduce the presence of voids. Once the adhesive had solidified, the specimen was removed from the mold and post-cured at 70 °C for a duration of four hours. Then, the joints were cut into 28 mm * 250 mm and both sides of the joints were polished. Additionally, to further guide the crack propagation direction, specimens were grooved on both sides, as shown in Figure 1b. Removed adhesive material has a right-triangle cross-section on both sides. The pre-crack was cut in two steps, first with a band saw and then the final 5 mm with a 0.125mm diameter diamond wire saw. In the end, piano hinges were attached to the specimens and the surface was then painted for DIC technique. Specimens were tested at 0.24 mm/min with an MTS Landmark servo-hydraulic testing machine, calibrated to 5 kN load capacity. Three classes of joints were manufactured with different void contents, i.e. low, medium, and high void contents. The joints with the lowest void content were manufactured by applying pressure on the adhesive (without level control usually performed by spacers), with the consequence that thickness control was not perfect. Due to the difficulty of manufacturing and the cutting procedure error, only one specimen with low void content was tested. The test matrix is given in Table 1. Joints with medium and high void content have uniform thickness. After the DCB tests, the void distribution of joints after tests was assessed by conducting 3D X-ray tomography (RX Solutions Ultratom) on the stable crack propagation area. AVIZO 3D software was used for epoxy and void segmentation and the void distribution reconstruction.

Sample type name	Sample size	Test Speed	Void content	Number of samples
VCL	Composite width 28 mm; Adhesive thickness 10 mm	0.24 mm/min	Low void content	1
VCM	Composite width 28 mm; Adhesive thickness 10 mm	0.24 mm/min	Medium void content	4
VCH	Composite width 28 mm; Adhesive thickness 10 mm	0.24 mm/min	High void content	4

Table 1: DCB test matrix.

2.2 Data reduction method

The SERR calculation method of thin DCB joints can be adapted for thick joints, including Single Beam Theory (SBT), Corrected Beam Theory (CBT) and Experimental Compliance Method (ECM) [18]. When using the single beam theory (SBT) method, the contribution of the adhesive layer to flexural rigidity is disregarded for thin adhesive joints, but becomes significant for thick adhesive joints. The calculation of flexural rigidity is based on the geometry of the arm, as depicted in Figure 2. The initial stage involves computing the neutral axis position ($\bar{z}$) and subsequently determining the flexural rigidity (EI). However, it is essential to note that the SBT method may yield imprecise results as it does not account for shear deflection, root rotation, and plastic zone deformation.

$$\bar{z} = \frac{\frac{E_c}{E_a} * A_c * \overline{z_c} + A_a * \overline{z_a}}{\frac{E_c}{E_a} * A_c + A_a} \tag{1}$$

$$EI = E_c * I_c + E_c * A_c * |\overline{z_c} - \bar{z}|^2 + E_a * I_a + E_a * A_a * |\overline{z_a} - \bar{z}|^2 \tag{2}$$

$$G_{SBT} = \frac{P^2}{2 * b} * \frac{dC}{da} = \frac{P^2 * a^2}{b * EI} \tag{3}$$

Here, the corner marker c and a are composite adherend and adhesive separately. E is the elastic modulus, A is the cross-section area and z the position of the center of gravity. Since CBT and ECM calculation considers the compliance of the whole beam, including the adhesive layer contribution, the adaption is not needed. The calculation formulas are shown in [18].

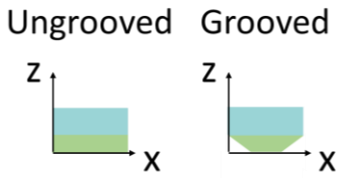

Figure 2: Schematic of one arm for flexural rigidity calculation.

The load-displacement (P-δ) prediction curves are calculated based on SBT and CBT. The curves are separated into two parts. The initiation curve before crack propagation is expected to have a linear relation. The other one is the propagation curve, where the crack length is expressed in terms of compliance and substituted into G calculation equation.

$$P = \frac{3 * EI * \delta}{2 * a_0^3} \tag{4}$$

$$P = \sqrt[4]{\frac{4 * EI * \bar{G}^3 * b_n^3}{9 * \delta^2}} \tag{5}$$

3 RESULTS AND DISCUSSION

3.1 VCL test results

Figure 3 shows the joint test results with low void content. As discussed, its thickness increases from 10 mm at the beginning to 14 mm at the end. Figure 3a shows the fracture surface, which contains a pre-crack region, a stable propagation region, and a fast separation region. The pre-crack region on the left was cut manually. The long middle part with light green color corresponds to the stable propagation. Unstable crack propagation (stick-slip crack propagation) and crack propagation deviation (crack kinking) only occurred when the two arms were completely separated. The load-displacement data is plotted in Figure 3b with the corresponding measured crack length.

Figure 3c illustrates the SERR curves derived by SBT, CBT, and ECM. SBT exhibits a rising trend, while the CBT results converge to the average value of 3.16 kJ/m^2. In contrast, ECM values tend to decrease after the crack starts to propagate. The thickness variation could be the reason for the increase in the SERR values in the final stages. Figure 3d shows the thickness influence on SERR calculation by assuming that the thickness of the joint is uniform. For comparison, the two SBT curves calculated with 10mm or 14mm adhesive thickness are compared in this figure. Around 20% decrease is observed when the thickness increases by 4 mm. Shivakumar et al. [21] performed sandwich DCB debonding tests to determine interfacial SERR values. They concluded that the ECM and CBT methods are appropriate when the crack length is less than half of the specimen length, which could be a contributing factor to the observed increase in SERR values at the end of our test.

The SBT and CBT prediction curves are given in Figure 3e. Equation 4 and 5 were used for the derivation of the prediction curves for all three test types. The displacement values are taken as the independent variable and the calculated load values are the dependent variable. The crack initiation region (equation 4) is linear. However, the linear prediction curves and the experimental results diverge significantly. The crack propagation region (equation 5) is predicted using average SERR values during stable propagation as one fixed parameter. The crack propagation region shows monotonically decreasing force with displacement. CBT prediction shows slight deviations from the experimental results, which can be explained by the fracture surface roughness, arc-shape crack, and the distribution of small voids and flaws. A significant offset between the SBT prediction and experimental curves can be observed.

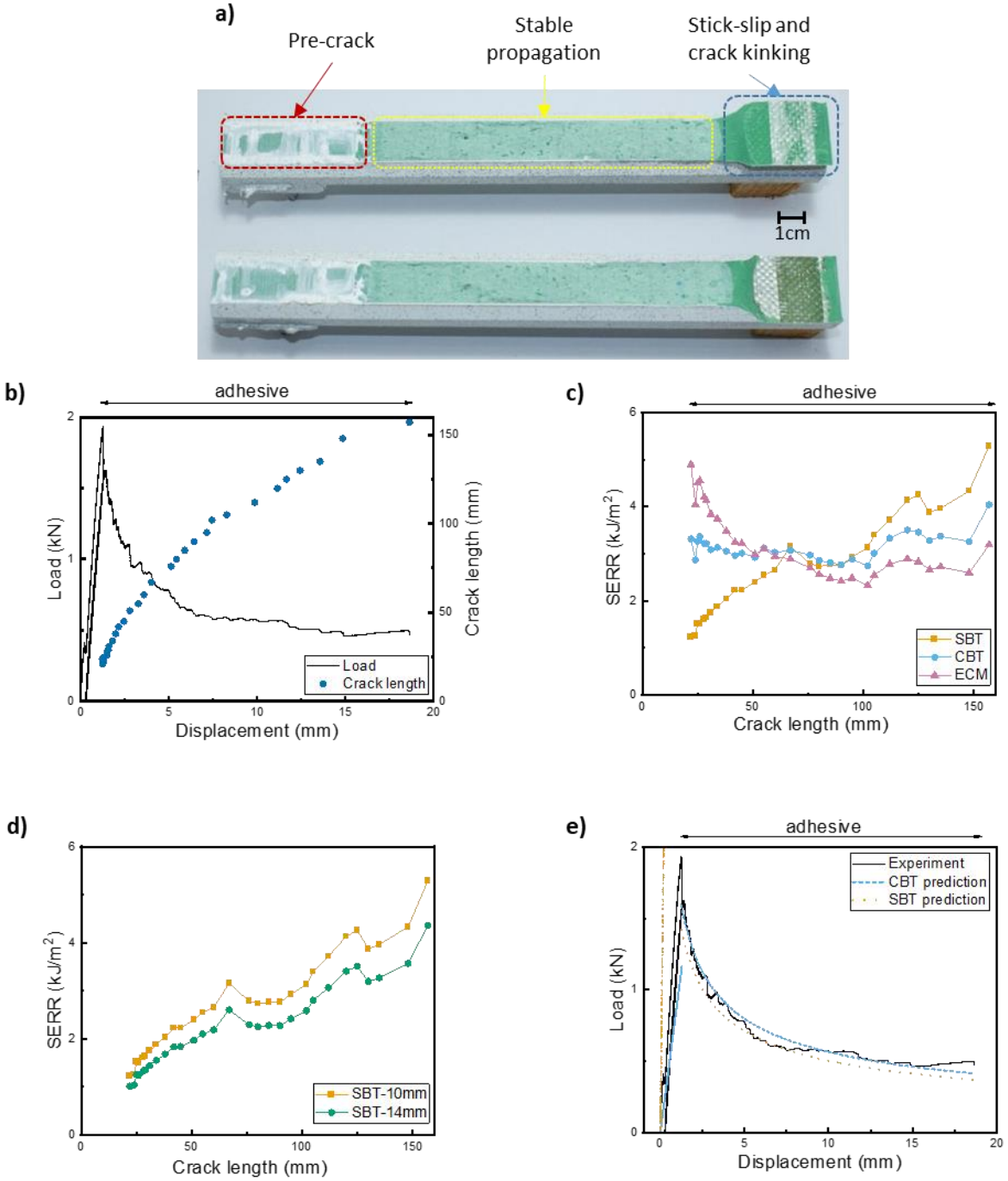

Figure 3: Results of VCL specimen: a) fracture surface after test b) corresponding load-displacement curve c) corresponding SERR curves d) SBT SERR curves with two different adhesive layer thickness e) prediction and experimental load-displacement curves.

3.2 VCM test results

Joints with medium void content (VCM specimens) have uniform thickness. The test results of one joint are shown in Figure 4. Inspecting the fracture surface (Figure 4a), many voids are observed and light green color and dark green color regions alternate, indicating that stick-slip took place several times. In total, five zones are observed, these are: the pre-crack region, first stable propagation region, first stick-slip propagation region and second stable and stick-slip propagation regions, from left to right. It is obvious that there is a void at the boundary of the first stick-slip propagation that corresponds to the

vertical line in the load-displacement curve (Figure 4b). After the first stick-slip crack propagation, the crack was arrested at the middle plane, so the crack could still propagate without path deviation. Finally, an unstable propagation went along the interface and broke the joint. Data obtained before the first stick-slip was used for the calculation. SERR curves are shown in Figure 4c, even though limited data is obtained before the first stick-slip propagation, the curve tendency is still similar to the previous result with low void content. SBT results are still much smaller than CBT and ECM. Increasing and decreasing trends are observed for SBT and ECM separately.

The average values (without considering the arrested SERR value) are used for deriving the prediction curve, which are plotted as dashed lines and compared with the experimental data in Figure 4d. The initiation prediction curves still differ from the experimental curves. As for the propagation prediction, CBT prediction and experimental curves agree to each other within the two stable propagation regions. The experimental curve restored and converged towards the prediction curve after the first stick-slip crack propagation. Using the results calculated from the first stable propagation part can properly predict the loading curve of the second stable propagation part. It can be concluded that the validation of the calculation theory is not affected by the stick-slip crack propagation. The joint with medium void content is still appropriate for the DCB static test.

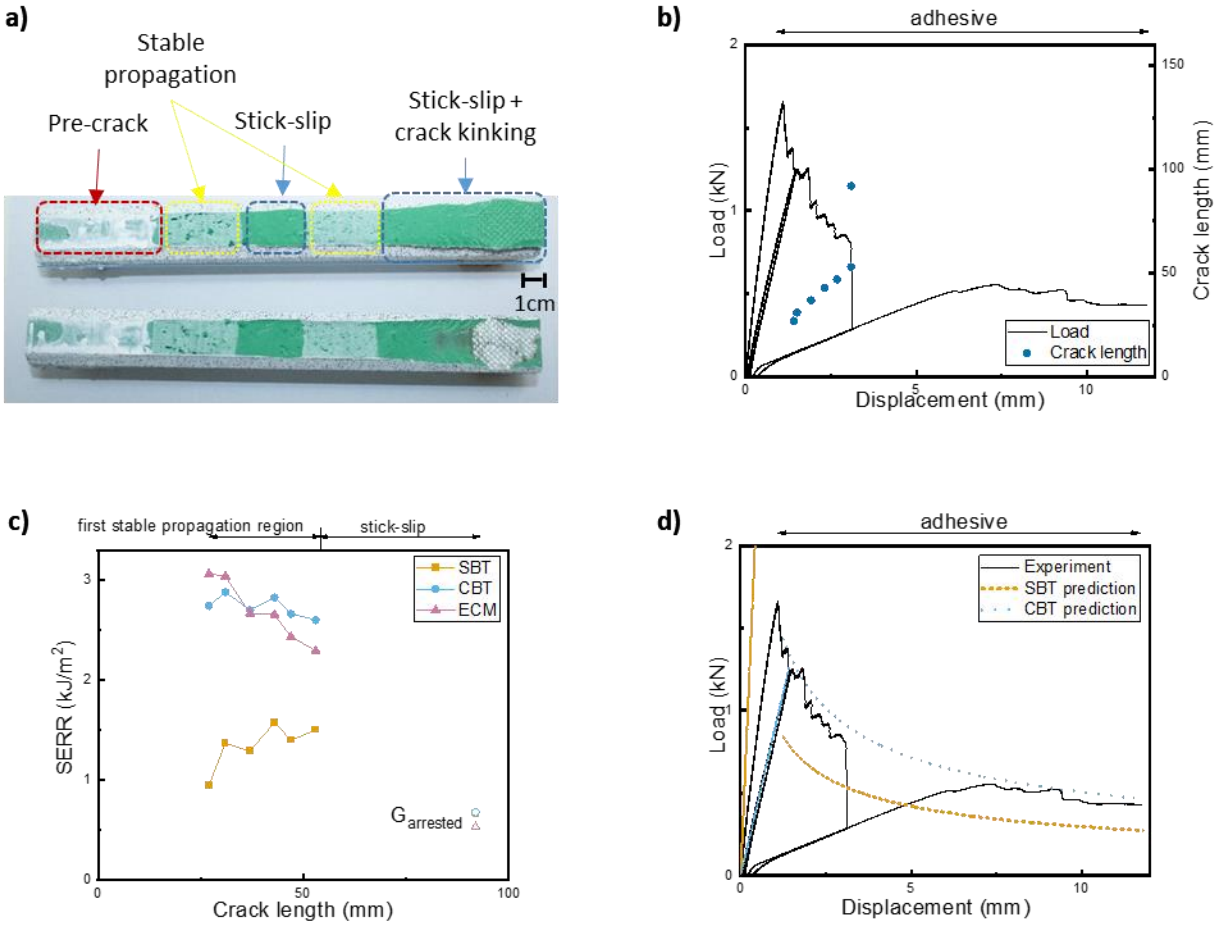

Figure 4: Results of VCM specimens: a) fracture surface after test, b) corresponding load-displacement curve, c) corresponding SERR curves, d) prediction and experimental load-displacement curves.

3.3 VCH test results

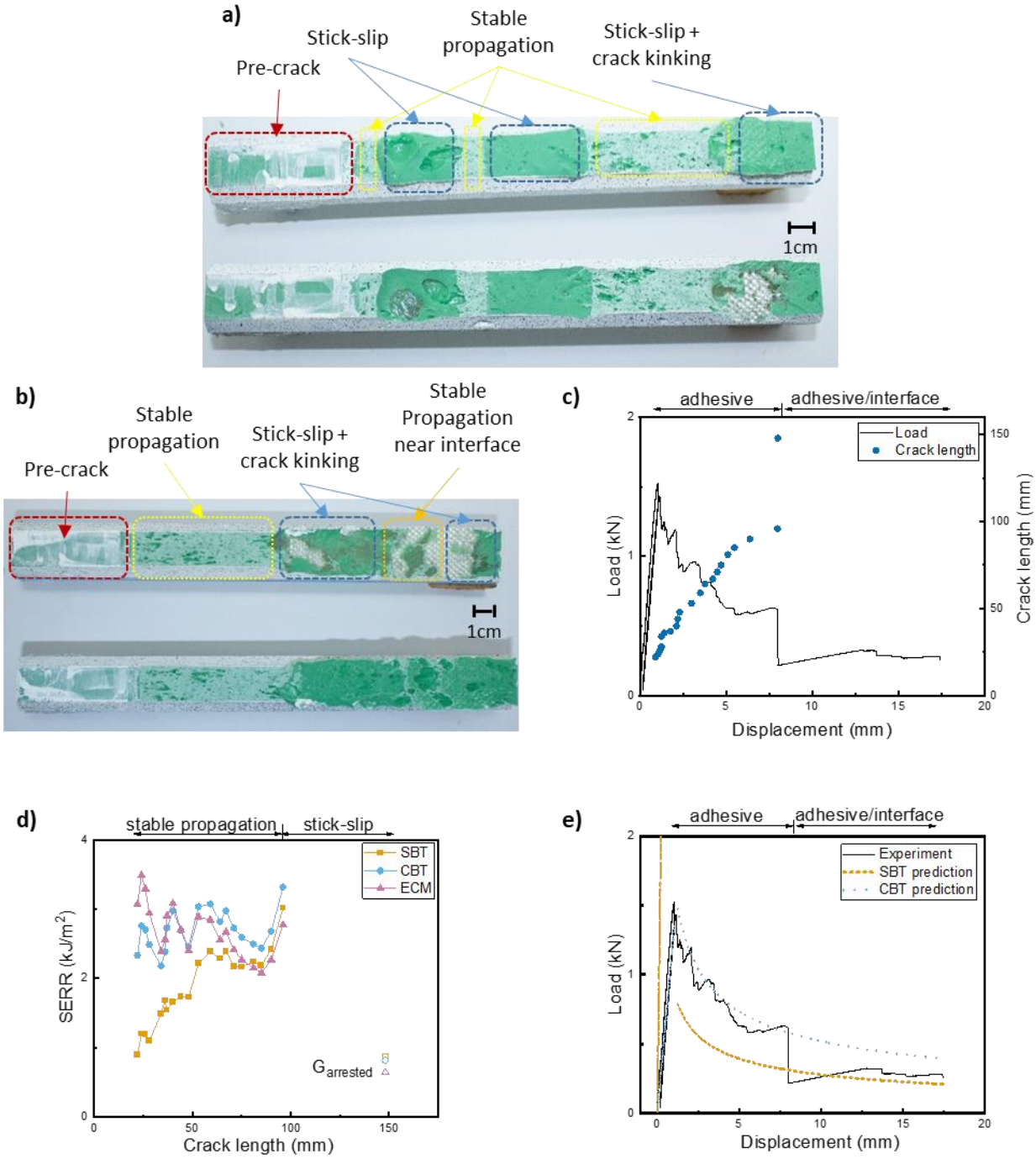

Figure 5: Results of VCH specimens: a) one fracture surface after test, b) another fracture surface after test, c) corresponding load-displacement curve, d) corresponding SERR curves, e) prediction and experimental load-displacement curves.

The fracture surface of joints with high void content is dominated by voids. Depending on the void size and distribution, different fracture behavior can be observed. When the crack tip encounters large voids, stick-slip crack propagation takes place, as shown in Figure 5a. Figure 5b depicts the alternative case, when the voids are not too large with proper shape, stable propagation can be achieved. In addition, the crack kinking direction can be inverted, which is obvious in Figure 5b. Fracture tends to choose the

crack path consuming less energy that contains voids, since the adhesive is already separated by the voids. The crack finally goes back to adhesive layer from the interface to the adhesive.

Since the second one (Figure 5b) has adequate stable propagation length, the related load-displacement curve, SERR calculation and prediction curves are plotted in Figure 5, using the data obtained before the first stick-slip. CBT is consistent with ECM data, while the progressive increased SBT data differ from the others. The curve depicting high void content fluctuates more compared with low void content results, and the valley values can be down to 2.3 kJ/m^2 between peaks close to the value found in the low void content case, which is around 3.1 kJ/m^2.

The prediction curves are shown as dashed lines Figure 5e. The initiation part still shows large deviation between prediction curves and experimental curves. Regarding the propagation part, the crack propagation prediction curve is calculated with the first peak SERR value, assuming that peak values are not influenced by voids. Comparing the CBT prediction and experimental data, the prediction curve links the peak values of the experimental data, which accords with the calculation assumption. Nevertheless, SBT prediction is much lower than the experimental curve.

3.4 Void content investigation

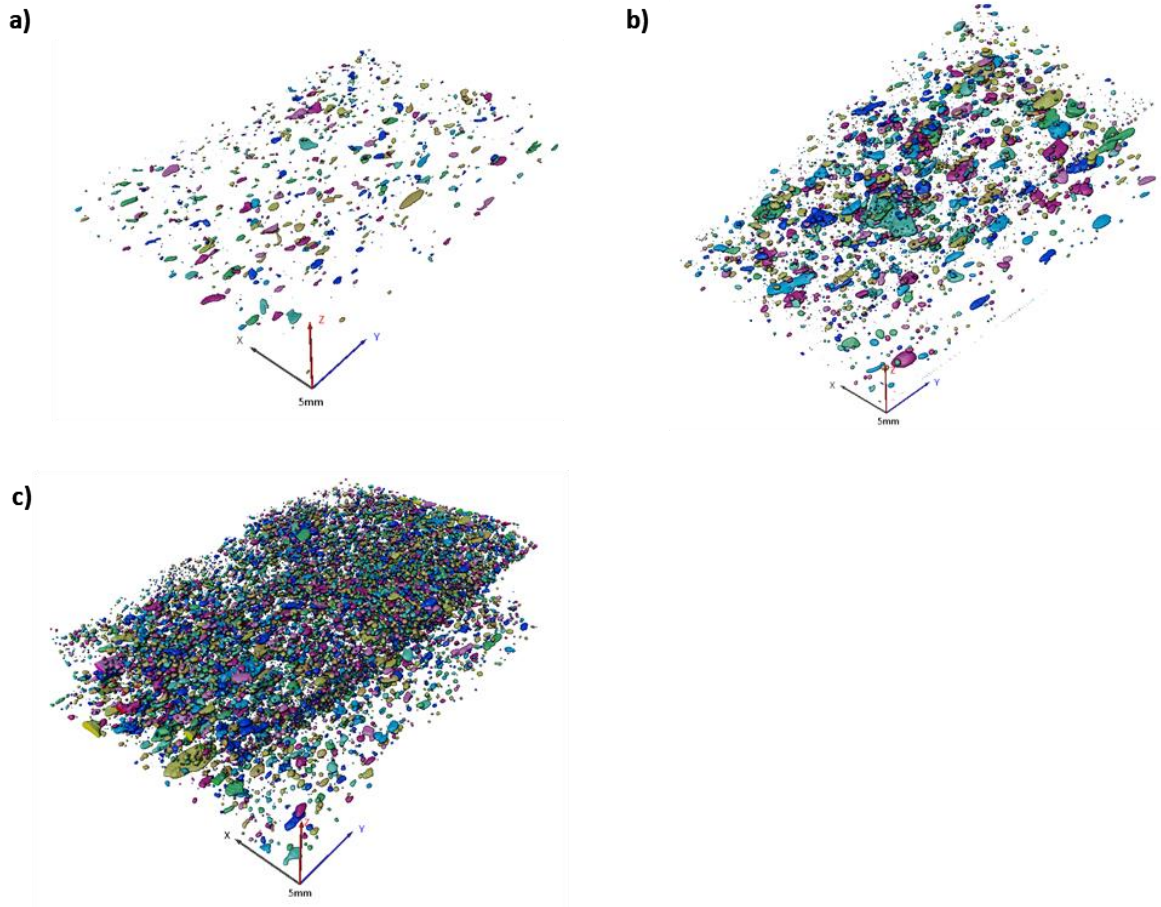

Figure 6: Void distribution reconstruction based on X-ray scanning results of three samples shown above after static test: a) VCL b) VCM c) VCH.

Figure 6 shows the void distribution of the three grooved samples shown above. Since the adhesive has a yield stress (adhesive cannot flow without external force), the adhesive was applied to completely cover the surface of the cavity using a scraper, causing the voids to align with the direction of application. This proves that the adhesive application step is critical to control the void content. To minimize the occurrence of large voids, it is advisable to apply the adhesive layer-by-layer and degassing it multiple times during the process.

Sample type name	Number of voids larger than 1mm^3	Number of voids larger than 0.1mm^3	Void volume percentage	Largest voids volume
VCL	0	33	0.36 %	0.75 mm^3
VCM	24	232	2.19 %	10.32 mm^3
VCH	20	587	4.13 %	9.87 mm^3

Table 2: Void content in three grooved samples shown above.

Void content information is shown in Table 2. Only voids inside the fractured samples were included in the analysis (the voids at the edge and fracture surface are excluded). The presence of larger voids is more common in high void content joints. It is obvious that void volume percent and the distribution of extremely large voids dominate the final results. The crack path goes through large voids and thus consumes less energy, and the existence of voids will influence the stress state ahead of the crack tip, so the crack has a high possibility to deviate from the middle plane of the joints. The combination of the two aforementioned reasons could lead to crack kinking. The grooved specimen follows the similar principle to confine the crack path, since the grooved plane has the smallest surface area, so ideally the crack propagation consumes the lowest energy by selecting the grooved path, whereas when the voids are too large, this lowest energy propagation path is replaced by the path with high void concentration and crack kinking occurs. Controlling the void volume lower than 2 % could help the fracture mechanics investigation. However, depending on the void distribution, joints with void volume percent higher than 4 % might experience crack kinking anytime throughout the test.

Large dimension voids are one main cause of the stick-slip crack propagation and the stability of the crack propagation can easily be affected by these large voids. It has already been proven that when the crack encounters voids, the plastic zone size is influenced and the crack growth rate changes [9]. Moreover, the SERR value drastically decreases since the surface area decreases, so the stable propagation cannot be maintained, some energy is dissipated into kinetic energy, triggering stick-slip crack propagation.

4 CONCLUSIONS

The void content within the adhesive layer considerably affects the quasi-static fracture behavior of thick-DCB joints. This research has provided a deeper insight into the void dominating fracture behavior. It showed that large voids ahead of the crack tip can lead to stick-slip crack propagation; afterwards, the joint behavior is unpredictable. Ideally, low void content is beneficial for stable crack propagation without crack kinking. Joints with 2 % voids within adhesive layer can still be tested with sufficient stable crack propagation length, while high void content is not recommended, since it can result in fluctuating SERR curve or more complicated behavior. The crack will prefer to choose the path with voids consuming less energy.

ACKNOWLEDGEMENTS

The authors acknowledge funding under the Lead Agency scheme from the Research Foundation - Flanders (FWO Vlaanderen) through the project grant G031020N and the Swiss National Science Foundation (SNF) through the project grant 200021E_18944/1 with the title "Combined numerical and experimental approach for the development, testing and analysis of thick adhesive joints in large wind turbine blades". The authors also acknowledge the experimental assistance provided by the technical team of the structural engineering experimental platform (GIS-ENAC at the Ecole Polytechnique Fédérale de Lausanne (EPFL), Switzerland), and Sika Technology AG for providing materials and support.

REFERENCES

[1] Wind Electricity – Analysis, *IEA*. https://www.iea.org/reports/wind-electricity (accessed Dec. 04, 2022).

[2] Wind Turbines: the Bigger, the Better, *Energy.gov*. https://www.energy.gov/eere/articles/wind-turbines-bigger-better (accessed Dec. 04, 2022).

[3] A. Memija, 123-Metre Wind Turbine Blade Rolls Out in China, *Offshore Wind*, Sep. 07, 2022. https://www.offshorewind.biz/2022/09/07/123-metre-wind-turbine-blade-rolls-out-in-china/ (accessed Dec. 04, 2022).

[4] R. Lopes Fernandes, M. K. Budzik, R. Benedictus, and S. Teixeira de Freitas, Multi-material adhesive joints with thick bond-lines: Crack onset and crack deflection, *Composite Structures*, **266**, Jun. 2021, pp. 113687, (doi: 10.1016/j.compstruct.2021.113687.)

[5] A. A. Bautista Villamil, J. P. Casas-Rodriguez, A. Porras Holguin, and M. Silva Barrera, Mode I Crack Propagation Experimental Analysis of Adhesive Bonded Joints Comprising Glass Fibre Composite Material under Impact and Constant Amplitude Fatigue Loading, *Materials*, **14**, no. 16, Jan. 2021, Art. no. p16, (doi: 10.3390/ma14164380.)

[6] M. N. Saleh, M. K. Budzik, M. Saeedifar, D. Zarouchas, and S. Teixeira De Freitas, On the influence of the adhesive and the adherend ductility on mode I fracture characterization of thick adhesively-bonded joints, *International Journal of Adhesion and Adhesives*, **115**, Jun. 2022, pp. 103123, (doi: 10.1016/j.ijadhadh.2022.103123.)

[7] P. L. Rosendahl, Y. Staudt, C. Odenbreit, J. Schneider, and W. Becker, Measuring mode I fracture properties of thick-layered structural silicone sealants, *International Journal of Adhesion and Adhesives*, **91**, Jun. 2019, pp. 64–71, (doi: 10.1016/j.ijadhadh.2019.02.012.)

[8] D3433, Test Method for Fracture Strength in Cleavage of Adhesives in Bonded Metal Joints, ASTM International, West Conshohocken (PA). (doi: 10.1520/D3433-99R20.)

[9] S. Heide-Jørgensen and M. K. Budzik, Effects of bondline discontinuity during growth of interface cracks including stability and kinetic considerations, *Journal of the Mechanics and Physics of Solids*, **117**, Aug. 2018, pp. 1–21, (doi: 10.1016/j.jmps.2018.04.002.)

[10] F. Sayer, *Sub-component testing for structural adhesive joint Assessment in Wind Turbine Rotor Blades*. Bremerhaven: Fraunhofer Verlag, 2020.

[11] A. Sengab and R. Talreja, A numerical study of failure of an adhesive joint influenced by a void in the adhesive, *Composite Structures*, **156**, Nov. 2016, pp. 165–170, (doi: 10.1016/j.compstruct.2015.12.052.)

[12] M. Shishesaz and S. Tehrani, The effects of circumferential voids or debonds on stress distribution in tubular adhesive joints under torsion, *The Journal of Adhesion*, **96**, no. 16, Dec. 2020, pp. 1396–1430, (doi: 10.1080/00218464.2019.1605598.)

[13] J. N. Rossettos, P. Lin, and H. Nayeb-Hashemi, Comparison of the Effects of Debonds and Voids in Adhesive Joints, *Journal of Engineering Materials and Technology*, **116**, no. 4, Oct. 1994, pp. 533–538, (doi: 10.1115/1.2904324.)

[14] P. Zuo and A. P. Vassilopoulos, Review of fatigue of bulk structural adhesives and thick adhesive joints, *International Materials Reviews*, **66**, no. 5, Jul. 2021, pp. 313–338, (doi: 10.1080/09506608.2020.1845110.)

[15] D. Griffin and M. Malkin, Lessons Learned from Recent Blade Failures: Primary Causes and Risk-Reducing Technologies, *49th AIAA Aerospace Sciences Meeting including the New Horizons Forum and Aerospace Exposition, Orlando, Florida, Jan. 2011*. (doi: 10.2514/6.2011-259.)

[16] A. I. M. Foletti, J. Sena Cruz, and A. P. Vassilopoulos, Fabrication and curing conditions effects on the fatigue behavior of a structural adhesive, *International Journal of Fatigue*, **139**, Oct. 2020, pp. 105743, (doi: 10.1016/j.ijfatigue.2020.105743.)

[17] D. E. Lees and A. R. Hutchinson, Mechanical characteristics of some cold-cured structural adhesives, *International Journal of Adhesion and Adhesives*, **12**, no. 3, Jul. 1992, pp. 197–205, (doi: 10.1016/0143-7496(92)90054-Y.)

[18] Y. Zhang, A. P. Vassilopoulos, and T. Keller, Mode I and II fracture behavior of adhesively-bonded pultruded composite joints, *Engineering Fracture Mechanics*, **77**, no. 1, Jan. 2010, pp. 128–143, (doi: 10.1016/j.engfracmech.2009.09.015.)
[19] ASTM D638, Test Method for Tensile Properties of Polymer Matrix Composite Materials, ASTM International, West Conshohocken (PA). (doi: 10.1520/D3039_D3039M-17.)
[20] ASTM D3039M-17, Test Method for Tensile Properties of Plastics, ASTM International, West Conshohocken (PA). (doi: 10.1520/D0638-14.)
[21] K. Shivakumar, H. Chen, and S. A. Smith, An Evaluation of Data Reduction Methods for Opening Mode Fracture Toughness of Sandwich Panels, *Jnl of Sandwich Structures & Materials*, **7**, no. 1, Jan. 2005, pp. 77–90, (doi: 10.1177/1099636205047085.)